Anti-3-^{18}F-FACBC (^{18}F-Fluciclovine) PET/CT of Breast Cancer: An Exploratory Study

Funmilayo I. Tade[1], Michael A. Cohen[1], Toncred M. Styblo[2], Oluwaseun A. Odewole[1], Anna I. Holbrook[1], Mary S. Newell[1], Bital Savir-Baruch[3], Xiaoxian Li[4], Mark M. Goodman[1], Jonathon A. Nye[1], and David M. Schuster[1]

[1]*Department of Radiology and Imaging Sciences, Emory University, Atlanta, Georgia;* [2]*Department of Surgery, Emory University, Atlanta, Georgia;* [3]*Department of Radiology, Loyola University Medical Center, Maywood, Illinois; and* [4]*Department of Pathology and Laboratory Medicine, Emory University, Atlanta, Georgia*

The purpose of this study was to explore the uptake of the synthetic amino acid analog PET radiotracer *anti*-3-^{18}F-FACBC (^{18}F-fluciclovine) in breast lesions with correlation to histologic and immunohistochemical characteristics. **Methods:** Twelve women with breast lesions underwent 45-min dynamic PET/CT of the thorax after intravenous administration of 366.3 ± 14.8 (337.44–394.05) MBq of ^{18}F-fluciclovine. Uptake in the primary lesions at 4 representative time points (5, 17, 29, and 41 min) after injection were correlated with histologic, imaging, and clinical findings. The significance of differences in SUV_{max} and tumor-to-background ratios between malignant and benign tissue were calculated. Correlations of activity to histologic and immunohistochemical cancer subtypes were made including Ki-67 intensity and Nottingham grade (NG). **Results:** There were 17 breast lesions (4 benign, 13 malignant) including 7 of 13 invasive ductal, 5 of 13 invasive lobular, and 1 of 13 metaplastic carcinomas. There was a significant difference in mean SUV_{max} ± SD of malignant (6.2 ± 3.2, 6.0 ± 3.2, 5.7 ± 2.8, and 5.6 ± 3.0) versus benign (1.3 ± 0.6, 1.2 ± 0.5, 1.2 ± 0.6, and 1.1 ± 0.5) lesions at 5, 17, 29, and 41 min, respectively (all $P \leq 0.0001$). Tumor-to-background (aorta, normal breast, and marrow) ratios were also significantly higher in malignant than benign breast lesions (all $P \leq 0.02$). The highest ^{18}F-fluciclovine activity seems to be present in triple-negative and NG3 subtypes. Across time points, quantitative Ki-67 had weak positive correlation with SUV_{max} ($R_1 = 0.48$ [$P = 0.03$], $R_2 = 0.44$ [$P = 0.03$], $R_3 = 0.46$ [$P = 0.03$], $R_4 = 0.43$ [0.06]). In 7 patients, ^{18}F-fluciclovine PET visualized locoregional and distant spread including that of lobular cancer, though identification of hepatic metastases was limited by physiologic background activity. **Conclusion:** The uptake characteristics of ^{18}F-fluciclovine are reflective of the histologic and immunohistochemical characteristics in suspected breast lesions with greater activity in malignant versus benign etiology. The data from this exploratory study may be useful to design future studies using ^{18}F-fluciclovine PET for breast tumor imaging as well as for detection of locoregional and distant spread.

Key Words: FACBC; fluciclovine; PET; breast cancer

Breast cancer is the most common cancer and the second leading cause of cancer-related deaths in women (*1*). Histologic and molecular characteristics of breast cancer have significant effects on therapeutic decisions as well as disease-free and overall survival (*2*). Mammography, ultrasound, and MRI form the backbone of breast imaging (*3–6*).

^{18}F-FDG PET has also assumed an important role in whole-body staging, recurrent disease detection, and therapy response monitoring (*7*). Molecular breast imaging with ^{18}F-FDG positron emission mammography and ^{99m}Tc-sestamibi are also being explored (*3,8,9*). These have limitations including differentiation of malignancy from posttherapy effects and challenges with certain histologic subtypes such as lobular cancer, which accounts for 10% of invasive breast cancers. Thus, molecular imaging targeting receptors or other aspects of the metabolome are under investigation (*8,9*). Because amino acid metabolism is upregulated in breast cancer, molecular imaging using natural or synthetic amino acid radiotracers is a potentially attractive approach (*9,10*).

Anti-1-amino-3-^{18}F-fluorocyclobutane-1-carboxylic acid (^{18}F-FACBC or ^{18}F-fluciclovine) is a synthetic amino acid analog transported via system L (L-type amino acid transporter 1 [LAT1]) and alanine/serine/cysteine transporter 2 (ASCT2) amino acid transporters and has shown promise in the imaging of prostate and other cancers (*11*). Liang reported ^{18}F-fluciclovine uptake in breast carcinoma cell lines, which correlated with malignant potential, as well as in orthotopic MDA-MB-231 breast carcinoma xenografts (*12*). In this study, we aimed to explore uptake of ^{18}F-fluciclovine in suspected breast lesions, report associations between uptake and histologic as well as immunohistochemical characteristics of breast carcinoma, and describe activity within locoregional or remote tumor spread.

MATERIALS AND METHODS

Patient Selection

The institutional review board at Emory University approved this study, which is Health Insurance Portability and Accountability Act–compliant, and all subjects signed a written informed consent form. Twelve female patients 18 y or older with breast lesions naïve to therapy and about to undergo biopsy or who were at least 1 wk postbiopsy were recruited and underwent ^{18}F-fluciclovine PET/CT between September 2012 and January 2015 (NCT01659645).

[18]F-Fluciclovine PET/CT Imaging

Preparation of ^{18}F-fluciclovine under Investigational New Drug Application 72,437 was completed via the FastLab Cassette System

(GE Healthcare) or via automated synthesis (13). All subjects fasted for at least 4 h to stabilize plasma amino acid levels (14). A CT of the thorax (80–120 mA; 120 kVp) was performed then, 366.3 ± 14.8 (337.44–394.05) MBq of ^{18}F-fluciclovine were injected intravenously, and a 45-min dynamic list-mode PET acquisition at 1 table position encompassing the primary breast lesions was completed in a Discovery 690 PET/CT scanner (GE Healthcare). Data were reconstructed into 4-min time frames and transferred to a MIMVista workstation (MIM Software) for analysis. Four patients also underwent clinical ^{18}F-FDG PET performed on the same scanner after intravenous injection of 439.84 ± 37 MBq of ^{18}F-FDG and an uptake time of approximately 60 min. Blood glucose ranged from 89 to 104 mg/dL in these patients. ^{18}F-Fluciclovine and ^{18}F-FDG scans were obtained at an average interval ± SD of 12 ± 8 d (range, 1–21 d).

Safety Evaluation

Vitals signs were monitored during and immediately after the ^{18}F-fluciclovine scan. Complete metabolic profile, complete blood count, and urinalysis just before and approximately 1 wk after the ^{18}F-fluciclovine PET scan were obtained, and no attributable adverse events were noted. Dosimetry and phase 1 safety data have already been reported (15–17).

Image Analysis

A board-certified nuclear radiologist unmasked to all correlative imaging and clinical information using the 3-dimensional PET-Edge tool and a custom workflow (MIM Software) drew target and background regions of interest. After the regions of interest were drawn, the values of the maximum voxel (SUV_{max}), average voxel (SUV_{mean}), and average of all voxels within a fixed spheric ROI of 1 cm^3 centered on the most metabolically active part of the lesion (SUV_{peak}) were recorded at representative time points of 5–8 min, 17–20 min, 29–32 min, and 41–44 min (referenced as 5, 17, 29, and 41 min in this article). The SUV_{mean} of background structures (blood pool at aortic arch, normal breast tissue and marrow at T5 vertebrae) were also measured using at least a 1-mL spheric region of interest best conforming to the background structure. For normal breast tissue, regions either contralateral or most distant from suspect lesions were chosen. Images were scrutinized for marker clips and, if present, were correlated to surgical reports for associations between imaging and histologic sampling. In ill-defined or multifocal breast lesions or in a nodal conglomerate, the most representative region was measured.

Histologic Analysis

Histologic examination of biopsy specimens was performed by a board-certified breast pathologist to evaluate the Nottingham grade (NG1, NG2, and NG3). Immunohistochemical analysis was performed for estrogen receptor (ER), progesterone receptor (PR), human epidermal growth factor receptor 2 (HER2), and Ki-67, using Dako's HERCEPTEST and MIB-1 kits, respectively. ER and PR expression was positive if 1% or more of the tumor nuclei were stained (18). HER2 was negative if staining was 0 or 1+, equivocal if 2+, and positive if 3+ per American Society of Clinical Oncology/College of American Pathologists guidelines. We analyzed HER2 equivocal cases by fluorescence in situ hybridization study to determine HER2 gene amplification. Ki-67 staining was scored as the number of positively stained nuclei as a percentage of the total tumor cells and reported in 3 categories: low, ≤10%; intermediate, >10% to <14%; and high, ≥14%.

Statistical Methods

A 2-tailed t test was used to compare the means of SUV_{max} in malignant with that of benign breast tumors and SUV_{max} of benign breast tumors with that of normal breast tissue across time points. ANOVA was used to compare the means of SUV_{max} of malignant lesions based on Nottingham grades, molecular subtypes, and Ki-67.

A Pearson correlation coefficient was used to determine the correlation between SUV_{max} and Ki-67 intensity (%) in malignant breast tumors. Correlation coefficient (R) was interpreted as very strong, 0.9–1.0; strong, 0.7 to −<0.9; moderate, 0.5 to −<0.7; weak, 0.3 to −< 0.5; and none, < 0.3. All P values were 2-sided and statistically significant if less than 0.05. Statistical analysis was done using IBM SPSS Statistics 22 and Microsoft Excel 2010.

RESULTS

Demographics

Twelve women (11 postmenopausal and 1 premenopausal) with an average age ± SD of 64 ± 12 y (range, 49–89 y) were recruited. At diagnosis, 9 of 12 patients had primary breast cancer, and 3 of 12 had local disease recurrence. In these 12 women, 17 breast lesions (13 malignant and 4 benign) were analyzed. Histologic verification was via ultrasound-guided core biopsy except for 1 benign lesion confirmed on conventional imaging. Six of 12 biopsies were done within 1 d after ^{18}F-fluciclovine PET/CT whereas 6 of 12 were done from 8–35 d before ^{18}F-fluciclovine PET/CT. Demographic details and results of histologic and immunohistochemical analysis are provided in Table 1.

^{18}F-Fluciclovine Kinetics

On the basis of full dynamic analysis, uptake of ^{18}F-fluciclovine peaked approximately 4 min after administration in 10 of 13 malignant lesions followed by a gradual clearance of 5%/min on average across these subjects. In the remaining 3 of 13 malignant lesions, the time to peak was the same, but the washout was substantially slower at 0.5%/min. There did not seem to be a relationship between these patterns and tumor subtype. Ratios of malignant lesions to the background structures of marrow and blood reached a plateau at between 6 and 10 min after administration. Malignant-to–normal breast tissue ratios decreased over time at 0.8%/min primarily because of a slower washout of normal tissue than of the malignant lesions.

^{18}F-Fluciclovine Activity and Histologic Characteristics of Breast Lesions

Malignant breast lesions had significantly higher uptake than benign lesions, with higher tumor-to-background ratios (Fig. 1; Table 2). SUV_{max} in benign breast lesions was not significantly different from that of normal breast tissue (Table 2). Figure 2 is an example of uptake in benign and malignant breast lesions.

Of the malignant lesions, there were 7 of 13 invasive ductal carcinoma (IDC), 5 of 13 invasive lobular carcinoma (ILC), and 1 of 13 invasive metaplastic carcinoma with sarcomatous differentiation (IMC). The mean SUV_{max} (±SD) for IDC was 7.7 ± 2.8, 7.5 ± 2.8, 7.0 ± 2.4, and 6.8 ± 2.8, and for ILC it was 3.8 ± 1.8, 3.9 ± 1.7, 3.8 ± 1.5, and 3.9 ± 1.5 at 5, 17, 29, and 41 min, respectively. Although ^{18}F-fluciclovine uptake in IDC and ILC were both higher than benign breast lesions ($P \le 0.01$ across time points), IDC had significantly higher uptake than ILC ($P \le 0.02$ across time points). Figure 3 is a scatterplot of IDC, ILC, and benign lesions. The IMC had an SUV_{max} of 8.6, 8.9, 8.9, and 9.1 across time points.

There were 3 of 12 NG1, 5 of 12 NG2, and 4 of 12 NG3 tumors. NG is not applicable to IMC. Except at the first time point, NG3 had significantly higher uptake than NG2 ($P = 0.06$, 0.03, 0.03, and 0.03) and NG1 ($P = 0.13$, 0.04, 0.03, and 0.03) (Table 3). There was no significant difference in uptake between NG1 and NG2.

TABLE 1
^{18}F-Fluciclovine Activity Correlated to Demographic, Histologic, and Immunohistochemical Characteristics

Subject no.	Age (y)	Location of breast lesion	Size (cm)	TNM	Histologic diagnosis	Ki-67 (%)	^{18}F-Fluciclovine uptake (SUV$_{max}$) (min)			
							5	17	29	41
1	63	RUO	1.5 × 1.2 × 1.0	T1cNxM0	IDC NG2; ER+/PR+/HER2−	High (21)	5.6	5.1	4.8	3.6
		RUI	Diffuse	NA	Stable posttherapy scar*	NA	1.2	1.4	1.5	1.4
2	50	RUI	2.5 × 2.0 × 0.3	NA	Ductal hyperplasia and columnar cells with microcalcifications	NA	2.0	1.8	1.8	1.5
3	67	LUI	1.1 × 1	T1N0M0	IDC NG1; ER+/PR+HER2−	High (29)	9.7	7.4	6.6	6.1
4	77	RUO	2.0	T1cN1aM0	IDC NG2; ER+/PR−/HER2+	Intermediate (11)	3.0	3.8	4.0	4.2
		RUO	0.7	NA	Fibroadipose tissue	NA	0.6	0.6	0.5	0.3
5	60	RLO	1.4 × 1.2 × 1.5	T1N0M0	ILC NG2; ER+/PR+/HER2−	High (45)	3.9	3.3	3.4	3.5
		LUI	3.2 × 1.5 × 1.9	T2N1M1	IDC NG3; ER+/PR−/HER2−	High (97)	7.9	8.3	8.2	8.2
6	54	RUI	15.1 × 14.7 × 15.2	T4cN1M0	IMC; ER−/PR−/HER2−	High (62)	8.6	8.9	8.9	9.1
		Left subareaolar	1.8	NA	Fibrocystic change, apocrine metaplasia, and focal ductal hyperplasia	NA	1.2	1.1	1.1	1.2
7	60	LLI	2.0 × 1.5 × 1.4	T1cN0M0	IDC NG3; ER+/PR−/HER2−	High (95)	7.5	6.2	5.4	5.0
8	89	LUO	3.0 × 2.8 × 2.1	T2N0M0	IDC NG3; ER+/PR+/HER2−	High (40)	8.8	9.3	9.3	9.3
		Right axillary tail	2.3 × 2.2 × 1.9	T2N0M0	IDC NG3; ER−/PR−/HER2−	High (34)	11.7	12.3	10.3	11.0
9	68	LUO	15.4	T3NxM0	ILC NG2; ER+/PR+/HER2−	High (39)	6.6	6.4	5.9	5.5
10	54	RUO	1.5	T1N1M0	ILC NG1; ER+/PR−/HER2−	High (15)	2.2	2.0	1.7	1.8
11	73	LUO	4 × 3.2 × 1.3	T2N0M0	ILC NG1; ER+/PR+/HER2−	Low (2)	2.6	3.2	3.4	3.6
12	49	LUO	5.5 × 4.6	T3N2aM0	ILC NG2; ER+/PR+/HER2−	High (25)	3.5	4.5	4.5	4.9

*Confirmed on conventional imaging.

RUO = right upper outer; NG = Nottingham grade; RUI = right upper inner; NA = not applicable; LLI = left lower inner; RLO = right lower outer; LUI = left upper inner; LUO = left upper outer.

^{18}F-Fluciclovine Activity and Immunohistochemical Characteristics of Malignant Breast Tumors

Tumors were classified into standard subtypes based on immunohistochemical analysis: triple-negative ($n = 2$), HER2-positive type (HER2+; $n = 1$), and ER-positive/HER2-negative type (ER+/HER 2− [PR-positive [PR+] or PR-negative [PR−]; $n = 10$) (19). Triple-negative breast tumors demonstrated the highest mean uptake, followed by ER+/HER2− and lowest uptake in HER2+ type though without overall significance likely due to small sample size (Table 3). Figure 4 shows differential activity in a patient with triple-negative and ER+/HER2− tumors. Ki-67 intensity demonstrated positive weak linear correlation (R$_{Time point}$) with SUV$_{max}$ with R$_1$ = 0.48 ($P = 0.03$), R$_2$ = 0.44 ($P = 0.03$), R$_3$ = 0.46 ($P = 0.03$), and R$_4$ = 0.43 ($P = 0.06$).

^{18}F-Fluciclovine PET/CT and Locoregional and Distant Metastases

Histologic sampling occurred in 9 locoregional lymph nodes (4 benign and 5 malignant). Of the malignant nodes, 3 were ILC and 2 were IDC. At 5, 17, 29, and 41 min, respectively, ILC nodes had mean a SUV$_{max}$ (±SD) of 6.2 ± 0.8, 5.4 ± 0.7, 4.8 ± 0.9, and 4.3 ± 0.7; IDC nodes had a mean SUV$_{max}$ of 3.3 ± 2.6, 3.4 ± 2.2, 3.7 ± 2.6, and 4.0 ± 2.5; and benign nodes had mean a SUV$_{max}$ of 1.5 ± 0.4, 1.0 ± 0.1, 0.9 ± 0.3, and 0.8 ± 0.3. Differences were not statistically significant, but sample size was small. Figure 5 shows ^{18}F-fluciclovine uptake in a biopsy-proven ILC metastasis to axillary node reported negative on outside MRI and ultrasound. No internal mammary or more distant nodes were identified on ^{18}F-fluciclovine or other imaging. In 1 patient, micrometastatic (≤2 mm) nodal disease was not detected on ^{18}F-fluciclovine imaging, and in another patient a benign sentinel node could not be correlated to imaging.

In 1 patient with stage IV breast cancer, left axillary and skeletal involvement were well visualized on ^{18}F-fluciclovine imaging but not enlarging hepatic metastases on CT. Mean ^{18}F-fluciclovine SUV$_{max}$ in 4 representative skeletal lesions was 11.1 ± 1.7, 10.5 ± 2.3, 9.6 ± 2.3, and 9.1 ± 1.7 across time points. Although SUV$_{max}$ in a representative liver lesion was 7.6, 9.2, 10.3, and 10.5 across 4 time points, these lesions appeared relatively photopenic due to more intense physiologic hepatic background.
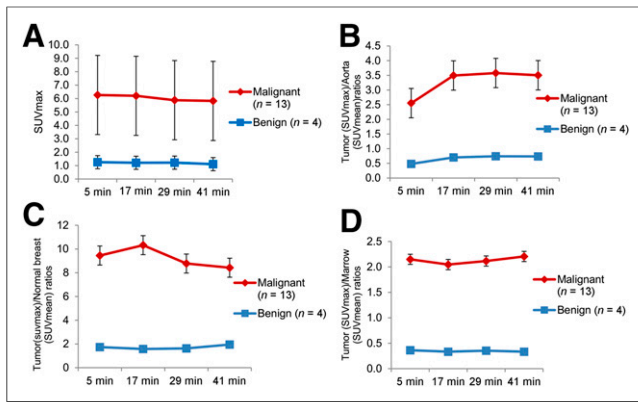
FIGURE 1. ^{18}F-Fluciclovine uptake in breast tumors (A), tumor-to-aorta ratios ($P < 0.002$) (B), tumor–to–normal breast ratios ($P < 0.0004$) (C), and tumor-to-marrow ratios ($P < 0.0001$) (D) in malignant compared with benign breast lesions.

^{18}F-Fluciclovine PET/CT Correlated with ^{18}F-FDG PET/CT

Four patients also underwent clinical ^{18}F-FDG PET/CT. ^{18}F-Fluciclovine and ^{18}F-FDG activity were compared in 8 biopsied lesions (5 malignant and 2 benign primary, 1 malignant node). The malignant lesions included 3 IDC, 2 ILC, and 1 IMC. For IDC, mean SUV$_{max}$ at 5 min with ^{18}F-fluciclovine was 8.7 ± 3.1 compared with 8.7 ± 4.2 for ^{18}F-FDG. For ILC, mean SUV$_{max}$ at 5 min with ^{18}F-fluciclovine was 4.6 ± 3.5 compared with 2.6 ± 1.0 for ^{18}F-FDG. Figure 6 is an example of uptake in an ILC

intramammary nodal metastasis on ^{18}F-fluciclovine and ^{18}F-FDG PET/CT imaging. In the IMC, ^{18}F-FDG had a higher uptake (SUV$_{max}$, 19.5) than ^{18}F-fluciclovine (SUV$_{max}$ 8.6 at 5 min) and both had similarly low activity in the necrotic center. For the benign breast lesions (fibrocystic change with focal ductal hyperplasia and posttherapy scar), SUV$_{max}$ on ^{18}F-fluciclovine imaging was 1.7 ± 0.7 at 5 min versus 2.1 ± 1.1 on ^{18}F-FDG. Differences between ^{18}F-fluciclovine and ^{18}F-FDG activity were not significant, but the sample size was small.

DISCUSSION

We set out to explore amino acid transport imaging using ^{18}F-fluciclovine in primary breast lesions and correlate our findings to histologic and immunohistochemical characteristics of breast cancer. Our results demonstrate higher uptake in malignant than benign breast lesions, with similarly low uptake in benign and normal breast tissue across all time points. ^{18}F-Fluciclovine activity also seemed to vary with histologic characteristics, hormone receptor status, and tumor grade, with higher uptake seen in triple-negative and NG3 breast cancers. ^{18}F-Fluciclovine uptake had weak positive correlation with Ki-67 intensity. Within the context of the small patient sample in this exploratory study, ^{18}F-fluciclovine PET visualized locoregional and distant spread except for hepatic metastasis secondary to physiologic hepatic uptake (11). In primary lesions, ^{18}F-fluciclovine activity in IDC seemed higher than in ILC, but the opposite was present with locoregional nodes. In addition, ^{18}F-fluciclovine activity was higher in ILC than ^{18}F-FDG. Though these observations

TABLE 2
^{18}F-Fluciclovine Uptake in Breast Lesions and Normal Breast Tissue

^{18}F-Fluciclovine PET/CT time points (min)	Status	Mean SUV$_{max}$ ± SD	Mean difference	Significance (2-tailed)
Malignant ($n = 13$) versus benign ($n = 4$) breast lesions				
5	Malignant	6.2 ± 3.2	4.9 (2.9–6.9)	0.0001
	Benign	1.3 ± 0.6		
17	Malignant	6.0 ± 3.2	4.8 (2.8–6.8)	0.0001
	Benign	1.2 ± 0.5		
29	Malignant	5.7 ± 2.8	4.5 (2.7–6.2)	<0.0001
	Benign	1.2 ± 0.6		
41	Malignant	5.6 ± 3.0	4.5 (2.6–6.3)	0.0001
	Benign	1.1 ± 0.5		
Benign breast lesions ($n = 4$) versus normal breast tissue ($n = 12$)				
5	Benign	1.3 ± 0.6	0.2 (−0.7–1.0)	0.7
	Normal	1.1 ± 0.7		
17	Benign	1.2 ± 0.5	0.1 (−0.7–0.9)	0.7
	Normal	1.1 ± 0.6		
29	Benign	1.2 ± 0.6	0.1 (−0.8–0.9)	0.9
	Normal	1.2 ± 0.6		
41	Benign	1.1 ± 0.5	0.3 (−0.5–1.1)	0.4
	Normal	0.8 ± 0.4		

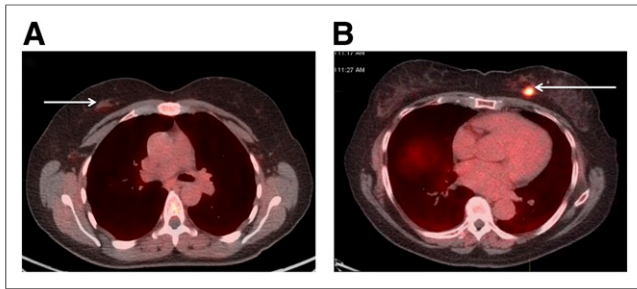Data in parentheses are 95% confidence intervals.

FIGURE 2. ^{18}F-Fluciclovine PET/CT images in benign ductal hyperplasia (arrow), SUV$_{max}$ at 5 min = 2.0 (A), and in IDC (arrow), SUV$_{max}$ at 5 min = 9.7 (B).

are based on limited data, further investigation of ^{18}F-fluciclovine PET in relation to ^{18}F-FDG PET and with a focus on lobular breast cancer seems warranted. Results of this exploratory trial can be used to guide further study design. Because lesion kinetics suggest that equilibrium is established quickly between malignant lesions and background structures, we believe that future trials should concentrate on the earlier time period after ^{18}F-fluciclovine injection.

Other metabolic activity upregulated in breast cancer includes that of amino acids. The amino acid transporters, specifically LAT1, ASCT2, ATB$^{0,+}$ SNAT1, and XCT, are overexpressed in breast cancer and reported to be associated with tumor growth, metastasis, and hormone receptor status (12,20–24). Our findings are similar to reports on amino acid PET imaging including L-[1-^{11}C]tyrosine and L-[methyl-^{11}C]methionine (MET), which reported higher uptake in malignant breast tumors than benign and background structures, with better tumor contrast on MET than ^{18}F-FDG (25,26). Yet, these radiotracers also have drawbacks, including incorporation into metabolic pathways and the 20-min half-life of ^{11}C necessitating proximity to a cyclotron. ^{18}F-Fluciclovine is a nonmetabolized synthetic amino acid–based PET radiotracer transported via LAT1 and ASCT2, with the advantage of the 110-min half-life of ^{18}F (11). We have previously reported on whole-body biodistribution of ^{18}F-fluciclovine and its potential utility in breast cancer (11,17,27).
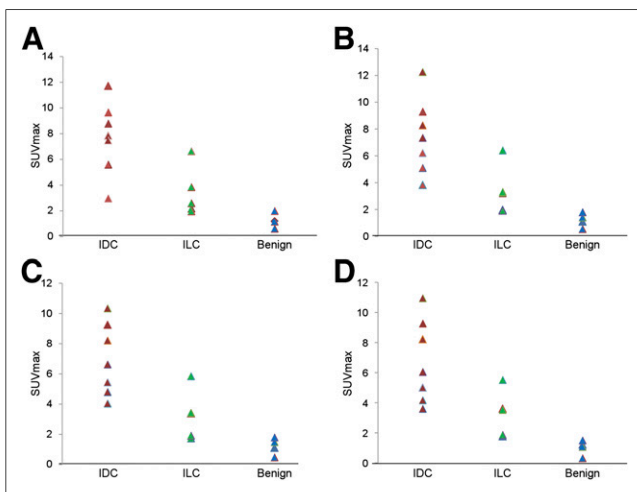
TABLE 3
^{18}F-Fluciclovine Uptake (SUV$_{max}$) Across Nottingham Grades and Receptor Status

Histologic characteristic	5 min	17 min	29 min	41 min
Nottingham grade (NG)				
NG1 (n = 3)	4.8 (±4.2)	4.2 (±2.8)	3.9 (±2.5)	3.8 (±2.2)
NG2 (n = 5)	4.2 (±1.9)	4.1 (±1.7)	4.0 (±1.5)	3.7 (±1.3)
NG3 (n = 4)	9.0 (±1.9)	9.0 (±2.5)	8.3 (±2.1)	8.4 (±2.5)
Receptor status				
TN (n = 2)	10.2 (±2.2)	10.6 (±2.4)	9.6 (±1.1)	10.0 (±1.3)
ER+/HER2− (n = 10)	5.8 (±2.7)	5.6 (±2.4)	5.3 (±2.3)	5.2 (±2.3)
HER2 type (n = 1)	3.0	3.8	4.0	4.2

TN = triple negative.

Though limited by small sample size, ^{18}F-fluciclovine demonstrated the greatest uptake with metaplastic cancer, followed by IDC, then ILC, with significantly higher mean ^{18}F-fluciclovine uptake in NG3 than in NG2 and NG1 breast cancers. There was also higher ^{18}F-fluciclovine uptake in triple-negative than ER+/HER2− and HER2+ breast cancers. These findings are similar to those reported with ^{18}F-FDG PET and indicate the more aggressive nature of triple-negative cancers (28,29). Shennan noted variation in expression of system L amino acid transporters in MDA-MB-231 (ER-negative [ER−]) and MCF-7 (ER+) breast cancer cell lines (30). Increased expression of ASCT2 has also been associated with prognostic indicators of breast cancer such as high-grade, ER−, PR−, triple-negative, and HER2+ breast cancers (23,31). We found significant but weak positive correlation between Ki-67 and ^{18}F-fluciclovine uptake across time points. Our findings are similar to our prior report of weakly positive though nonsignificant correlation between Ki-67 and ^{18}F-fluciclovine uptake in lung cancer (32). Similar findings have also been reported in a meta-analysis of Ki-67 and ^{18}F-FDG in breast cancer (33).

Limitations of this study include the small sample size and limited distribution across molecular subtypes and Ki-67. Not
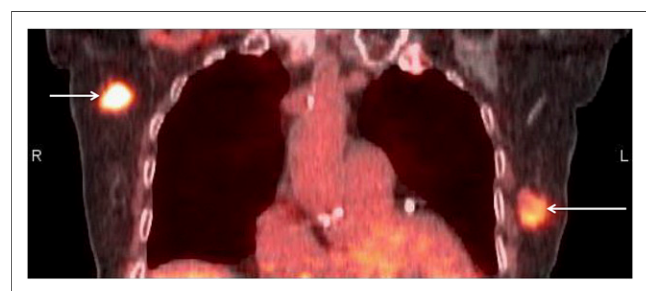

FIGURE 3. ^{18}F-Fluciclovine uptake in IDC, ILC, and benign breast lesions at 5 (A), 17 (B), 29 (C), and 41 (D) min.

FIGURE 4. ^{18}F-Fluciclovine PET/CT image in bilateral breast cancer showing higher uptake (SUV$_{max}$ at 5 min = 11.7) in triple-negative IDC on right (arrow) compared with uptake (SUV$_{max}$ at 5 min = 8.8) in ER+/HER2− IDC on left (arrow).
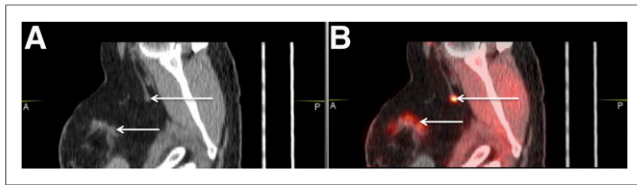
FIGURE 5. CT (A) and ^{18}F-fluciclovine PET/CT (B) images in left ILC. SUV$_{max}$ at 5 min = 3.5 in primary mass (short arrow) and 5.6 in biopsy-proven metastasis to a 6×11 mm left axillary lymph node (long arrow).
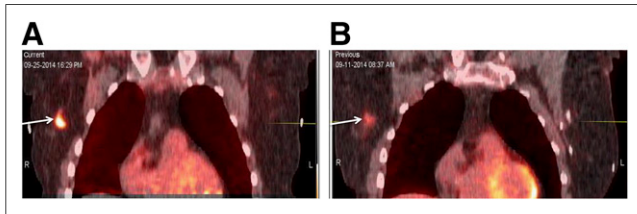

FIGURE 6. Higher uptake on ^{18}F-fluciclovine (SUV$_{max}$ at 5 min = 7.1) (A) than ^{18}F-FDG (SUV$_{max}$ = 3.3) (B) PET/CT imaging in 2.1×1.1 cm right ILC metastasis (arrow) to an intramammary lymph node.

all types of benign lesions such as fibroadenomas or fat necrosis were studied. Observations on the detection of metastatic disease or comparison to ^{18}F-FDG PET are preliminary. This exploratory study was designed to concentrate on dynamic uptake characteristics in primary lesions, and only 1 imaging bed position was acquired. The use of a whole-body PET/CT device for study of primary breast lesions limits observation for small lesions and results in underestimation of SUV. Partial-volume correction was not done. Positron emission mammography would be useful for further study but is not widely available. Six patients underwent ^{18}F-fluciclovine PET/CT after biopsy, but inflammation was likely mitigated because at least 8 d passed between the procedure and imaging. Though we reported SUV$_{max}$ for target structures, overall similar conclusions were made using SUV$_{mean}$ and SUV$_{peak}$ (Supplemental Figs. 1 and 2; Supplemental Table 1 [supplemental materials are available at http://jnm.snmjournals.org]).

CONCLUSION

In this exploratory study, ^{18}F-fluciclovine had a significantly higher uptake in malignant than benign breast lesions and normal breast tissue. ^{18}F-Fluciclovine activity seemed to vary with histologic and immunohistochemical characteristics of malignant breast tumors and demonstrated highest uptake in breast cancers, with poor prognostic factors. Further studies correlating whole exome RNA sequencing and amino acid transporter expression to ^{18}F-fluciclovine uptake in breast lesions are ongoing. Larger trials to determine the potential clinical benefits of ^{18}F-fluciclovine PET for staging, determination of therapy response, and diagnostic performance compared with conventional imaging and ^{18}F-FDG PET are required.

DISCLOSURE

The costs of publication of this article were defrayed in part by the payment of page charges. Therefore, and solely to indicate this fact, this article is hereby marked "advertisement" in accordance with 18 USC section 1734. Mark M. Goodman and Emory University

REFERENCES

1. DeSantis CE, Fedewa SA, Goding Sauer A, Kramer JL, Smith RA, Jemal A. Breast cancer statistics: convergence of incidence rates between black and white women. *CA Cancer J Clin.* 2016;66:31–42.
2. Mohamed A, Krajewski K, Cakar B, Ma CX. Targeted therapy for breast cancer. *Am J Pathol.* 2013;183:1096–1112.
3. Fowler AM. A molecular approach to breast imaging. *J Nucl Med.* 2014;55:177–180.
4. Glunde K, Jacobs MA, Pathak AP, Artemov D, Bhujwalla ZM. Molecular and functional imaging of breast cancer. *NMR Biomed.* 2009;22:92–103.
5. Drukteinis JS, Mooney BP, Flowers CI, Gatenby RA. Beyond mammography: new frontiers in breast cancer screening. *Am J Med.* 2013;126:472–479.
6. Gore JC, Manning HC, Quarles CC, Waddell KW, Yankeelov TE. Magnetic resonance in the era of molecular imaging of cancer. *Magn Reson Imaging.* 2011;29:587–600.
7. Groheux D, Espie M, Giacchetti S, Hindie E. Performance of FDG PET/CT in the clinical management of breast cancer. *Radiology.* 2013;266:388–405.
8. O'Connor M, Rhodes D, Hruska C. Molecular breast imaging. *Expert Rev Anticancer Ther.* 2009;9:1073–1080.
9. Schuster DM, Halkar RK. Molecular imaging in breast cancer. *Radiol Clin North Am.* 2004;42:885–908.
10. Plathow C, Weber WA. Tumor cell metabolism imaging. *J Nucl Med.* 2008;49 (suppl 2):43S–63S.
11. Schuster DM, Nanni C, Fanti S, et al. Anti-1-amino-3-^{18}F-fluorocyclobutane-1-carboxylic acid: physiologic uptake patterns, incidental findings, and variants that may simulate disease. *J Nucl Med.* 2014;55:1986–1992.
12. Liang Z, Cho HT, Williams L, et al. Potential biomarker of L-type amino acid transporter 1 in breast cancer progression. *Nucl Med Mol Imaging.* 2011;45:93–102.
13. McConathy J, Voll RJ, Yu W, Crowe RJ, Goodman MM. Improved synthesis of anti-[^{18}F]FACBC: improved preparation of labeling precursor and automated radiosynthesis. *Appl Radiat Isot.* 2003;58:657–666.
14. Isohashi K, Shimosegawa E, Kato H, et al. Optimization of [^{11}C]methionine PET study: appropriate scan timing and effect of plasma amino acid concentrations on the SUV. *EJNMMI Res.* 2013;3:27.
15. Asano Y, Inoue Y, Ikeda Y, et al. Phase I clinical study of NMK36: a new PET tracer with the synthetic amino acid analogue anti-[^{18}F]FACBC. *Ann Nucl Med.* 2011;25:414–418.
16. McParland BJ, Wall A, Johansson S, Sorensen J. The clinical safety, biodistribution and internal radiation dosimetry of [^{18}F]fluciclovine in healthy adult volunteers. *Eur J Nucl Med Mol Imaging.* 2013;40:1256–1264.
17. Nye JA, Schuster DM, Yu W, Camp VM, Goodman MM, Votaw JR. Biodistribution and radiation dosimetry of the synthetic nonmetabolized amino acid analogue anti-^{18}F-FACBC in humans. *J Nucl Med.* 2007;48:1017–1020.
18. Umemura S, Kurosumi M, Moriya T, et al. Immunohistochemical evaluation for hormone receptors in breast cancer: a practically useful evaluation system and handling protocol. *Breast Cancer.* 2006;13:232–235.
19. Groheux D, Majdoub M, Sanna A, et al. Early metabolic response to neoadjuvant treatment: FDG PET/CT criteria according to breast cancer subtype. *Radiology.* 2015;277:358–371.

20. Jager PL, Vaalburg W, Pruim J, de Vries EG, Langen KJ, Piers DA. Radiolabeled amino acids: basic aspects and clinical applications in oncology. *J Nucl Med.* 2001;42:432–445.

21. Karunakaran S, Ramachandran S, Coothankandaswamy V, et al. SLC6A14 (ATB0,+) protein, a highly concentrative and broad specific amino acid transporter, is a novel and effective drug target for treatment of estrogen receptor-positive breast cancer. *J Biol Chem.* 2011;286:31830–31838.

22. Shennan DB, Thomson J. Inhibition of system L (LAT1/CD98hc) reduces the growth of cultured human breast cancer cells. *Oncol Rep.* 2008;20:885–889.

23. Kim S. Kim do H, Jung WH, Koo JS. Expression of glutamine metabolism-related proteins according to molecular subtype of breast cancer. *Endocr Relat Cancer.* 2013;20:339–348.

24. Wang K, Cao F, Fang W, et al. Activation of SNAT1/SLC38A1 in human breast cancer: correlation with p-Akt overexpression. *BMC Cancer.* 2013;13:343.

25. Leskinen-Kallio S, Nagren K, Lehikoinen P, Ruotsalainen U, Joensuu H. Uptake of ^{11}C-methionine in breast cancer studied by PET: an association with the size of S-phase fraction. *Br J Cancer.* 1991;64:1121–1124.

26. Kole AC, Nieweg OE, Pruim J, et al. Standardized uptake value and quantification of metabolism for breast cancer imaging with FDG and L-[1-^{11}C]tyrosine PET. *J Nucl Med.* 1997;38:692–696.

27. Tade F, Odewole O, Cohen M, et al. Preliminary findings of anti-[^{18}F] FACBC (FACBC) PET-CT imaging of breast cancer (abstract). *J Nucl Med.* 2015;56(suppl 3):567.

28. Basu S, Chen W, Tchou J, et al. Comparison of triple-negative and estrogen receptor-positive/progesterone receptor-positive/HER2-negative breast carcinoma using quantitative fluorine-18 fluorodeoxyglucose/positron emission tomography imaging parameters: a potentially useful method for disease characterization. *Cancer.* 2008;112:995–1000.

29. Groheux D, Majdoub M, Tixier F, et al. Do clinical, histological or immunohistochemical primary tumour characteristics translate into different ^{18}F-FDG PET/CT volumetric and heterogeneity features in stage II/III breast cancer? *Eur J Nucl Med Mol Imaging.* 2015;42:1682–1691.

30. Shennan DB, Thomson J, Barber MC, Travers MT. Functional and molecular characteristics of system L in human breast cancer cells. *Biochim Biophys Acta.* 2003;1611:81–90.

31. van Geldermalsen M, Wang Q, Nagarajah R, et al. ASCT2/SLC1A5 controls glutamine uptake and tumour growth in triple-negative basal-like breast cancer. *Oncogene.* October 12, 2015 [Epub ahead of print].

32. Amzat R, Taleghani P, Miller DL, et al. Pilot study of the utility of the synthetic PET amino-acid radiotracer anti-1-amino-3-[^{18}F]fluorocyclobutane-1-carboxylic acid for the noninvasive imaging of pulmonary lesions. *Mol Imaging Biol.* 2013;15:633–643.

33. Deng SM, Zhang W, Zhang B, Chen YY, Li JH, Wu YW. Correlation between the uptake of ^{18}F-fluorodeoxyglucose (^{18}F-FDG) and the expression of proliferation-associated antigen Ki-67 in cancer patients: a meta-analysis. *PLoS One.* 2015;10:e0129028.